IOP Publishing J. Phys. Commun. 3 (2019) 025004 https://doi.org/10.1088/2399-6528/ab0231

Journal of Physics Communications

CrossMark

OPEN ACCESS

RECEIVED
15 October 2018

REVISED
15 January 2019

ACCEPTED FOR PUBLICATION
28 January 2019

PUBLISHED
6 February 2019

PAPER

Frictionless mobility of submicron particles in model viscid fluid

J Stanek[1], P Fornal[2] and K Dziedzic-Kocurek[1]

[1] Marian Smoluchowski Institute of Physics, Jagiellonian University, Prof. S. Łojasiewicza 11, 30-348 Cracow, Poland
[2] Institute of Physics, Cracow University of Technology, Podchorążych 1, 30-083 Cracow, Poland

E-mail: Jan.Stanek@uj.edu.pl

Keywords: brownian motion, viscosity, mössbauer spectroscopy, diffusion

Abstract

The mechanism of inter- and intracellular diffusional transport by vesicles in living organisms is poorly understood at the molecular scale. The diffusion of submicron and nanoparticles in dense media has been treated by numerous theoretical models. We face this problem experimentally using Mössbauer spectroscopy. On a characteristic for this method narrow time scale ($\approx 10^{-7}$ s), the velocity distribution of 120 nm spherical Fe_2O_3 particles suspended in a 60% water solution of sucrose was determined by analyzing the ^{57}Fe Mössbauer spectral line profile. The particles usually exhibit classical Brownian motion, but their main diffusion mechanism is related to infrequent ($f \approx 10^6$ s^{-1}) but distant ($d \approx 1$ nm) translations. During such movements, the particles experience a minimal friction described by the temporal local viscosity, $\eta_{loc} \approx 28$ μPa·s.

Introduction

The mobility of submicron objects in viscous media, which is a key problem in some areas of nanotechnology and the main factor responsible for inter- and intracellular transport, is poorly understood at the atomic scale. The Einstein–Smoluchowski approach to the Brownian motion refers to free particles in an ideal gas [1, 2] but does not adequately explain the migration of massive particles. The high rate of biochemical processes in colloids has been explained by the concept of local viscosity [3], and molecular dynamics simulations have elucidated the role of the protein concentration on the lateral mobility of lipid membranes [4]. Recent developments in experimental methods have enabled the determination of the trajectories of particles composing living cells [5, 6] (for a review, see also [7]); the results suggest the abnormal nature of diffusion, which is frequently discussed in terms of fractional Brownian motion or continuous-time random walks (CTRWs) [8]. Nevertheless, the question of how, if at all, these models may be distinguished experimentally at the truly microscopic level remains open [9]. Indeed, three qualitatively different types of diffusion, namely diffusion constrained by elastic force, walking confined diffusion and hop diffusion were described in [10] leading to the similar mean square displacements.

We address this challenge by studying a model system composed of 120 nm spherical Fe_2O_3 particles suspended in a 60% water solution of sucrose. This particle size is characteristic of intracellular organelles or extracellular vesicles, which store and transport cellular biochemical products [7]. The dynamic viscosity (η) at 20 °C, $\eta = 58.5$ mPa·s [11], is very close to the average viscosity of mammalian cytoplasm (~50 mPa·s) [12].

Methods

The model system is composed of 120 nm spherical Fe_2O_3 particles suspended in a 60% water solution of sucrose. The obtained suspension was further atomized at 60 °C in an ultrasonic washer operating at a modulated frequency. To eliminate the remaining precipitates of the particles, the suspension was held at room temperature for a few hours; in the subsequent experiments, the supernatant fluid was taken.

In such a condensed solution, an amorphous sucrose hydrogen bond network is formed [13], and this honey-like matter should be described as a fluid plastic rather than a colloidal liquid. The estimated

concentration of the particles was less than 3.9 μm^{-3}, and the average interparticle distance was 635 nm; thus, the particles may be treated as noninteracting [14]. Each Fe_2O_3 particle contains 1.7×10^7 Fe_2O_3 molecules with a total atomic mass of 2.72×10^9 Da. Their chemical properties are identical with those of a bulk material, and the chemical inactivity enables the preparation of suspensions that are stable over many days. As Fe_2O_3 particles, we used the red pigment BAYFERROX® 120 (CAS No. 1309-37-1). According to the producer's technical specification [15], the predominant size of the spherical particles is 120 nm, the α-Fe_2O_3 content is greater than 97.1%, the molar weight is 159.7, and a water-soluble content is maximum 0.5%.

^{57}Fe Mössbauer spectroscopy was applied as the experimental method. The Mössbauer spectra were recorded in the transmission geometry using a WissEl spectrometer. The temperature-dependent spectra were collected in 1024 channels for one day, and the high-quality room temperature spectra were measured over 5 days in 4096 channels (before folding). For the temperature-dependent measurements, a bath WissEl cryostat was used, and the sample was placed vertically in the gas exchange chamber. The temperature variation was less than 0.1 K, and the inhomogeneity of the temperature over the sample area was less than 1 K. The velocity scale was calibrated using the α-Fe foil standard. Because the line profile analysis may be influenced by the nonlinearity of the nonresonant background of the spectrum owing to geometrical effects, a preliminary measurement was performed in the identical geometry with a blank (iron-free) absorber having a nonresonant absorption coefficient under the conditions used for the studied specimen. This procedure made background correction possible.

The Mössbauer spectra were evaluated using the WissEl program WinNormos-for-Igor. First, the nonresonant background from the dummy spectrum was fitted by a quadratic polynomial to determine its deviation from linearity. This correction was included as a fixed parameter for further spectral fitting. Next, the hyperfine parameters (hyperfine field B, isomer shift versus metallic iron IS, and quadrupole shift QS) of Fe_2O_3 particles pressed in a powder pellet were determined by standard Lorentzian line fitting. These parameters were used to fit the spectra of the Fe_2O_3 particles in suspension.

Results and discussion

For decades, according to Singwi and Sjolander [16] and Bonchev *et al* [17], the main measurable parameter was the line broadening ($\Delta\Gamma$) of the resonant Lorentzian absorption line of particles exhibiting Brownian motion. Recently, this approach was applied to the study of particle-matrix interaction in anisotropic medium [18] or in hydrogels [19].

The line broadening in ferrofluids may also arise from the Néel relaxation [20–22]. In the studied case, Fe_2O_3 particles are antiferromagnetic or weakly ferromagnetic. The size dependence of the superparamagnetic relaxation time of Fe_2O_3 particles with diameter between d ~6 to 27 nm is described in [23]. Accordingly, for 120 nm particles the Néel relaxation at room temperature is excluded. Certainly, the fast (in comparison to the life time of the 14.4 keV nuclear level) Brownian rotation of the particles might cause the broadening of the Mössbauer line due to the averaging of the magnetic hyperfine field but this would be connected wit the reduction of the observed Zeeman splitting in Mössbauer spectra which was not the case. Thus the entire line broadening is due to the translational Brownian motion.

In the Mössbauer energy unit (mm/s), where 1 mm $s^{-1} = 5 \times 10^{-8}$ eV, $\Delta\Gamma$ equals

$$\Delta\Gamma[\mathrm{mm/s}] = \frac{E_0^2 k}{3\pi\hbar c^2 r}\left(\frac{T}{\eta}\right) = 1.06 \times 10^{-10}\frac{T[K]}{r[\mathrm{m}]\eta[\mathrm{Pa}\cdot\mathrm{s}]} \tag{1}$$

where $E_0 = 14.41$ keV is the gamma radiation energy, r is the particle radius and T is the temperature. According to the uncertainty principle, this line broadening occurs because the movement of the particles limits the time period during which recoil-free absorption is possible. In our case, a relatively large mass of particles, $M = 4.5 \times 10^{-18}$ kg, is crucial. The recoil energy (E_R) intercepted by the entire particle, which is related to nuclear absorption of the gamma radiation by the ^{57}Fe nuclei, is approximately 100 times smaller than the Heisenberg line width, $\Gamma = 4.7 \times 10^{-9}$ eV, of the corresponding nuclear level:

$$E_R = \frac{E_0^2}{2Mc^2} = 4.1 \times 10^{-11}\ \mathrm{eV} \tag{2}$$

Thus, recoil-free nuclear absorption of the gamma radiation (the Mössbauer effect) may appear even for an unbounded free particle. This differs from the results of previous studies of many other smaller objects [24, 25]. The specimen studied here should be treated as a set of classical macroscopic absorbers. The feasibility of using Mössbauer spectroscopy to study the velocity distribution in such systems was noted half a century ago [26]. Because the recoil-free absorption cross section of the gamma radiation depends, via the Doppler effect, on the relative velocity (v–V) between the source of the radiation (v) and the absorbing particles (V) in the direction of

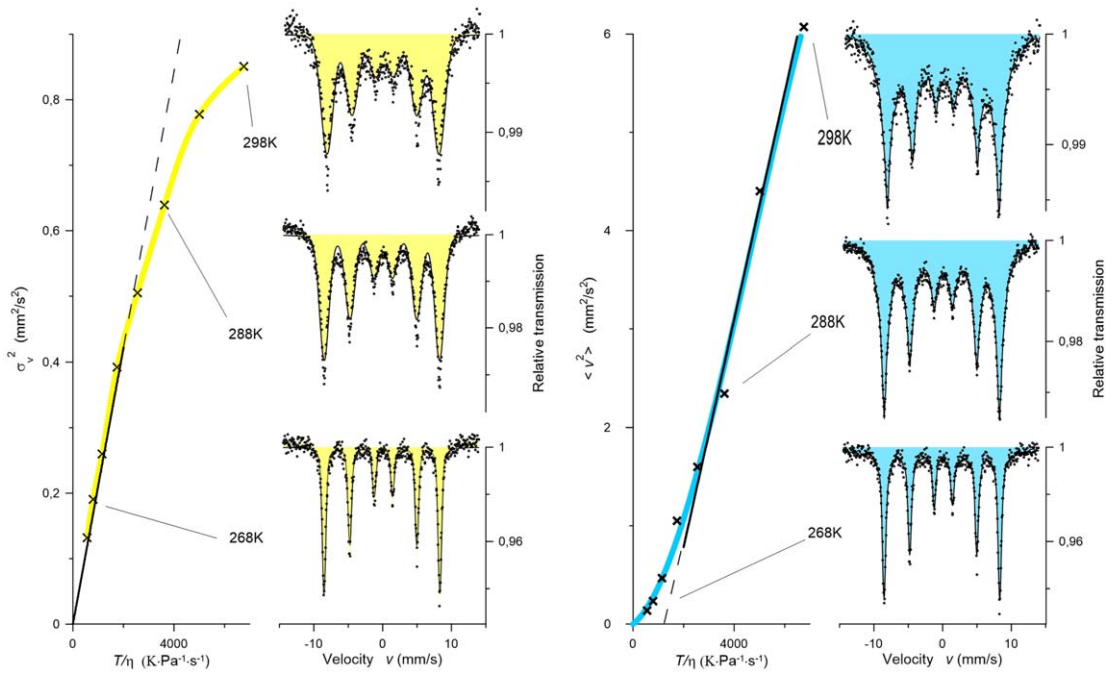

Figure 1. Selected Mössbauer spectra of 120 nm Fe_2O_3 particles in 60% water solution of sucrose recorded at various temperatures and their velocity distribution variance plotted versus (T/η). Left: Spectra fitted with a Gaussian distribution of $p(v)$ with the variance σ_V^2 as an adjustable parameter. Note the significant misfit above 283 K and the related deviation from linearity of the σ_V^2 versus (T/η) relation. Right: Spectra fitted with the model-independent distribution of $p(v)$. Note that the $\langle v^2 \rangle$ versus (T/η) relation deviates from linearity below 283 K.

the gamma radiation (both in the laboratory frame), the profile of the absorption line $I(v)$ is given by

$$I(v) = \int p(V) L(v - V) dV \tag{3}$$

where L is the Lorentzian function, and $p(V)$ is the velocity distribution of the nanoparticles [17]. Here, the particle velocity, $V = \Delta x/\tau$, is its mean value observed within a time τ of 141 ns, which is the lifetime of the 14.4 keV nuclear level, and Δx is the particle displacement during that time. Equation (3) illustrates the aim of this work: from the measured line profile $I(v)$, we may deconvolute the $p(V)$ distribution that describes the particle motion.

According to Einstein's theory, the one-dimensional displacement variance, σ_x^2, of a randomly wandering particle of radius r in a liquid of viscosity η after time τ is equal to $2D\tau = \sigma_x^2 = 2kT\tau/6\eta\pi r$, where D is a diffusion coefficient. Consequently, the variance of the velocity, σ_V^2, may be written as

$$\sigma_V^2 = \frac{k}{3\pi r\tau}\left(\frac{T}{\eta}\right) \tag{4}$$

Interestingly, in this case σ_V, which is a measure of the line broadening, is proportional to $\sqrt{\frac{T}{\eta}}$, in contrast to equation (1), where $\Delta\Gamma \sim \left(\frac{T}{\eta}\right)$. To test this relation, the Mössbauer spectra were recorded at 263–298 K, as shown on the left side of figure 1. We first assumed that the $p(V)$ distribution has a Gaussian profile; thus, we fitted the spectra with the Voigt lines to determine σ_V^2. The fits are clearly imperfect, but the linear dependence of σ_V^2 versus $\left(\frac{T}{\eta}\right)$ is conserved up to 283 K. The η values for the solution at each temperature were adopted from [10]. The diameter of the particles determined from the linear fit is $2r = 92(10)$ nm, which is comparable to the real particle size of 120 nm.

This agreement is astonishing when we consider that the Einstein–Smoluchowski theory was developed for free particles obeying a Maxwellian velocity distribution. Formal application of this classical theory leads to the following conclusions. According to the Stokes law, a particle exponentially loses velocity with a relaxation time $\tau_r = m/6\pi\eta r = 6.8 \times 10^{-11}$ s, which is comparable to the period of biomolecular vibrations. The corresponding average one-dimensional free path d of the particle equals $\langle |v| \rangle \tau_r$. For $\langle |v| \rangle = 24$ mm s^{-1}, as calculated from the Maxwell distribution, $d = 1.6 \times 10^{-12}$ m, which is 1.3×10^{-5} times the particle diameter and less than the typical amplitude of atomic vibrations in solids. For random one-dimensional jump model diffusion, the diffusion coefficient D is $d^2/2\tau_0$, where τ_0 is the average period between jumps. This expression for

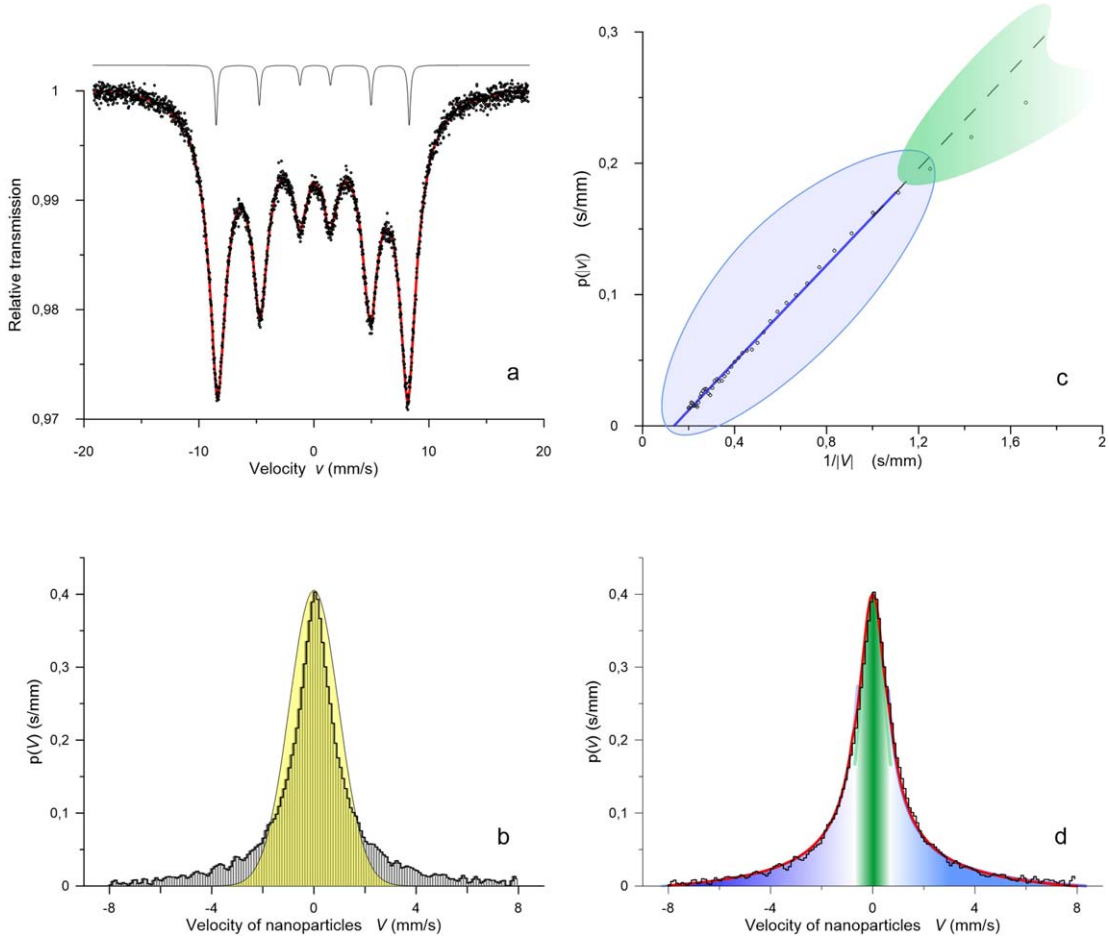

Figure 2. Analysis of Mössbauer line shape in the spectrum of 120 nm particles suspended in 60% water solution of sucrose at 295 K. (a) High-quality ^{57}Fe room-temperature Mössbauer spectrum. Solid line: fit assuming model-independent distribution of particle velocities in the direction of the gamma beam. For comparison, the spectrum of Fe_2O_3 nanoparticles in a dry pellet is shown (above). (b) Distribution of particle velocity $p(V)$ (bars). Solid line: best Gaussian approximation (yellow). (c) High-velocity range of $p(V)$ versus $1/V$. Solid line: linear fit. (d) Final fit of $p(V)$ composed of the central Gaussian distribution (green) and $1/V$ tail (blue).

D become identical to that derived by Einstein, $D = 6 \times 10^{-14}$ m^2 s^{-1}, if $\tau_r = \pi\tau_0$. Thus, during an observation time τ of 141 ns, the particles make about 6,500 random steps. Consequently, the particle displacements and velocity distribution measured within this time window should have a perfect Gaussian form, as observed in the dynamic light scattering and nanoparticle tracking analysis techniques, for which, however, the observation time is significantly longer [27].

The values of τ_0 and d might be related to the short-range random motion of a nanoparticle around its equilibrium position in a dense and viscous environment, which is known as bounded or restricted diffusion but which cannot explain its long-range migration. Indeed, above 283 K, the relation σ_V^2 versus (T/η) is observed to deviate from linearity, as shown on the left side of figure 1. This deviation is clearly related to the misfit in the fitted spectra when the Gaussian $p(V)$ profile is assumed.

To study the $p(V)$ profile in detail, we remeasured the Mössbauer spectrum of the system at 295 K but with much higher accuracy; see figure 2(a). The spectrum was fitted with sets of up to 161 sextets without assuming any functional form of $p(V)$. The normalized $p(V)$, which is shown in figure 2(b), does not reveal a Gaussian profile, that is, the relevant fit. A similar non-Gaussian velocity distribution of iron-bearing organic macromolecules was observed by Mössbauer spectroscopy three decades ago [25] and interpreted as the result of slow motions, which were attributed to the dynamics of the internal structures of the molecules and described in terms of overdamped harmonic oscillations. To the best of our knowledge, these phenomena have not been confirmed by any other experiment to date. In contrast, our results indicate that this unexpected slow but long-range motion involves the entire particle. This finding necessitates some modification of the classical theory. We postulate that in the studied case within the observation time window, $\tau = 141$ ns, the 'instantaneous' velocity of a particle is probed rather than its random walk behavior.

The observed velocity V depends on the sampling time t, which is a random variable; the probability density is $p(t) = 1/\tau_0$, where τ_0 is the average period between subsequent jumps. For decelerating particles,

$V(t) = V_0 e^{-\frac{t}{\tau_r}}$ and $t(V) = -\tau_r \ln\left(\frac{V}{V_0}\right)$, where V_0 is the average initial velocity. The probability density $p(V)$ within the range $V_0 \exp\left(-\frac{\tau_0}{\tau_r}\right) < V < V_0$ is

$$p(V) = \left| \frac{d[t(V)]}{dV} \right| p(t) = \frac{\tau_r}{\tau_0}\frac{1}{V} \tag{5}$$

If τ is comparable to τ_r, the measured initial velocity is reduced from its original value by a factor of $\frac{\tau_r}{\tau}\left[1 - \exp\left(-\frac{\tau}{\tau_r}\right)\right]$, but the functional relation of $p(V)$ remains unchanged. Interestingly, for a particle moving according to the relation $V(t) = V_0 \exp\left(-\frac{t}{\tau_r}\right)$, $\langle v^2 \rangle$ equals

$$\langle v^2 \rangle = \left| \int_{V_0}^{V_0 \exp\left(-\frac{\tau_0}{\tau_r}\right)} p(V) V^2 dV \right| = \int_{V_0 \exp\left(-\frac{\tau_0}{\tau_r}\right)}^{V_0} \frac{\tau_r}{\tau_0} V dV$$
$$= \frac{\tau_r}{2\tau_0} V_0^2 \left[1 - \exp\left(-\frac{\tau_0}{\tau_r}\right)\right] \sim \left(\frac{\tau_r}{2\tau_0}\right) {V_0}^2 \tag{6}$$

and for $\tau_r \gg \tau_0$, it is proportional to $1/\eta_{\mathrm{loc}}$ if $\tau_r = \frac{m}{6\pi\eta_{loc} r}\tau_0$, as in the case described by equation (4), where η_{loc} is the local temporal viscosity, which is a measure of the retarding force acting on the particle during the jump.

Figure 2(c) shows $p(V)$ versus $1/V$, which indeed exhibits linear dependence for $\sim$0.7 mm s^{-1} $< V <$ 5 mm s^{-1}. The V_0 value obtained by fitting is 7.4(3) mm s^{-1}, and τ_0/τ_r is 5.4(1), which indicates that particle jumps are infrequent.

It is not feasible to determine the absolute value of τ_r. Nonetheless, because we *do* observe the particle's movement within the time window τ, τ_r must be either longer than or at least comparable to τ ($\tau_r \geqslant \tau$). In further estimations, we assume the *lower* limit for $\tau_r \approx \tau = 141$ ns. In this case, the actual average initial velocity, $V_0/(1 - e^{-1}) = 11.7$ mm s^{-1}, is half the Maxwell value of the corresponding free particle. Consequently, the average jump distance d is 1.6 nm, which is much larger than the size of a water molecule ($\sim$0.28 nm) [28] but is comparable to the size of the sucrose molecule (1.09 nm) [29]. Further, the period between jumps, τ_0, is $\sim$764 ns. These values of d and τ_0 are $\sim$1000 and $\sim$35,000 times higher, respectively, than the corresponding values expected from the Einstein–Smoluchowski model. Consequently, the local diffusion coefficient (1.7×10^{-11} m^2 s^{-1}) is more than 35 times the value determined from the Einstein equation. Finally, the *temporal* viscosity, $\eta_{\mathrm{loc}} = m/6\pi r\tau_r \approx 28$ μPa·s, is comparable to the viscosity of air at room temperature at normal pressure ($\sim$18 μPa·s) [30] and is about 2×10^3 times smaller than the macroscopic viscosity [11]. Thus, the movement of the particle during the jump is nearly frictionless. Quite recently, such varying friction fluctuations have been rigidly formally related to the spatially correlated noise, which in some cases may lead to the formation of frictionless regions [31].

The $p(V)$ distribution for $0 < |V| < 0.4$ mm s^{-1} was fitted by a Gaussian function. In the remaining intermediate region, 0.4 to 0.6 mm s^{-1}, $p(V)$ was calculated as the difference between the $p(V)$ extrapolated from the high-velocity region and the Gaussian distribution. The particles are usually bounded, exhibiting very limited but frequent displacement, resulting in the Gaussian profile of $p(V)$, as expected from the Einstein–Smoluchowski model with $\sigma_V^2 = 0.15$ mm^2 s^{-2}; see figure 2(d). The total experimental $\langle v^2 \rangle$ value is 3.85(5) mm^2 s^{-2}. (Note that we distinguish σ_V^2 for the Gaussian distribution from $\langle v^2 \rangle$ for the model-independent fit.) Thus, bounded diffusion contributes less than 4% to the total diffusion at room temperature; the migration of submicron particles should be assigned to long-range displacements.

After the same numerical procedure was applied to determine $p(V)$ from the spectra measured at different temperatures, the $\langle v^2 \rangle$ versus (T/η) plot was constructed (figure 1, right), which exhibits linear dependence above 283 K. Below this temperature, the contribution of bounded diffusion to $\langle v^2 \rangle$ is substantial. The crossing point of the $\langle v^2 \rangle$ versus (T/η) line, where the T/η axis is at $T/\eta = 1000$, indicates that long-range jumps emerge at $T > 275$ K and $\eta < 300$ mPa·s.

Conclusions

In summary, in a straightforward experiment, we proved that an observation time of 141 ns may be short enough to monitor individual translation of submicron particles in a viscous solution. The particles reveal rare ($\sim$1 ms^{-1}), distant ($\sim$1 nm) frictionless jumps. We qualitatively assigned the possibility of these jumps to Smoluchowski's concept of local fluctuations of the number of colloidal molecules near a massive particle. Such a fluctuation liberates the particle, which adopts a velocity close to that expected from the Maxwellian distribution. Our result is consistent with the CTRW model [7] but is observed in the time mode; the tracks

inside a trap correspond to the Gaussian distribution of $p(V)$, and the jumps between traps are seen as the $p(V) \sim 1/V$ distribution assigned to decelerating particles. The simplicity of the applied numerical model, as well as the limited accuracy of the method, influence the accuracy of our estimations of the microscopic parameters. Nevertheless, because these parameters differ by a few orders of magnitude from those arising from the classical theory, which is already more than 100 years old, we are convinced that this work elucidates the main features of the Brownian motion of submicron particles in a viscid ambient. In our opinion, this depiction of the motion of submicron particles may provide hints for resolving the mystery of high-speed transport processes in living organisms; the cellular organelles are no longer passive targets for diffusing biomolecules but may actively explore their environment along the fluctuating local viscosity gradient.

ORCID iDs

J Stanek https://orcid.org/0000-0001-5108-7175

References

[1] Einstein A 1905 On the movement of small particles suspended in stationary liquids required by the molecular-kinetic theory of heat *Ann. Phys.* **17** 549
[2] Smoluchowski M 1906 Zur kinetischen theorie der brownschen molekularbewegung und der suspensionen *Ann. Phys.* **21** 756
[3] Szymański J, Patkowski A, Gapinski J, Wilk A and Holyst R 2006 Diffusion and viscosity in a crowded environment: from nano- to macroscale *J. Phys. Chem.* B **110** 25593
[4] Javanainen M, Martinez-Seara H, Metzler R and Vattulainen I 2017 Diffusion of integral membrane proteins in protein-rich membranes *J. Phys. Chem. Lett.* **8** 4308
[5] Metzler R, Jeon J H, Cherstvy A G and Barkai E 2014 Anomalous diffusion models and their properties: non-stationarity, non-ergodicity, and ageing at the centenary of single particle tracking *Phys. Chem. Chem. Phys.* **16** 24128
[6] Xu Q, Feng L, Sha R, Seeman N C and Chaikin P M 2011 Subdiffusion of a sticky particle on a surface *Phys. Rev. Lett.* **106** 228102
[7] Fuliński A 2017 Fractional brownian motions: memory diffusion velocity, and correlation functions *J. Phys. A: Math. Theor.* **50** 054002
[8] Burov S, Jeon J H, Metzler R and Barkai E 2011 Single particle tracking in systems showing anomalous diffusion: the role of weak ergodicity breaking *Phys. Chem. Chem. Phys.* **13** 1800
[9] Saxton M J 2012 Wanted: a positive control for anomalous subdiffusion *Biophys.* J **103** 2411
[10] Piskorz T and Ochab-Marcinek A 2014 A universal model of restricted diffusion for fluorescence correlation spectroscopy *The Journal of Phys. Chem.* B **118** 4906
[11] Swindells J F, Snyder C F, Hardy R C and Golden P E 1958 Viscosities of sucrose solutions at various temperatures: table of recalculated values *United States Department of Commerce, Supplement to the National Bureau of Standards* **440** 2
[12] Bicknese S, Periasamy N, Shohet S B and Verkman A S 1993 Cytoplasmic viscosity near the cell plasma membrane: measurement by evanescent field frequency-domain microfluorimetry *Biophys.* J **65** 1272
[13] Molinero V, Cagin T and Goddard W A III 2003 Sugar, water and free volume networks in concentrated sucrose solutions *Chem. Phys. Lett.* **377** 469
[14] Dziedzic-Kocurek K, Fornal P and Stanek J 2015 Mobility of interacting inorganic nanoparticles *Nukleonika* **60** 19
[15] Technical Data Sheet 2018 BAYFERROX 120, Lanxess GmbH, http://bayferrox.com/en/products-applications-bfx/product-search/bayferrox-120/
[16] Singwi K S and Sjolander A 1960 Resonance absorption of nuclear gamma rays and the dynamics of atomic motions *Phys. Rev.* **120** 1093
[17] Bonchev T, Aidemirski P, Mandzhukov I, Nedyalkova N, Skorchev B and Strigachev A 1966 A study of Brownian motion by means of the Mössbauer effect *Soviet Phys. JETP* **23** 42
[18] Hsia Y F, Fang N, Widatallah H M, Wu D M, Lee X M and Zhang J R 2010 Brownian motion of suspended particles in an anisotropic medium *Hyperfine Interact.* **126** 401
[19] Landers J, Roeder L, Salamon S, Schmidt A M and Wende H 2015 Particle-matrix interaction in cross-linked PAAM-hydrogels analyzed by Mössbauer spectroscopy *J. Phys. Chem.* C **119** 20642
[20] Landers J, Salomon S, Remmer H, Ludwig F and Wende H 2016 Simultaneous Study of Brownian and Néel Relaxation Phenomena in Ferrofluids by Mössbauer Spectroscopy *Nano Lett.* **16** 1150
[21] Gabbasov R *et al* 2019 Study of brownian motion of magnetic nanoparticles in viscous media by Mossabuer spectroscopy *JMMM* **475** 146
[22] Chuev M A, Cherepanov V M, Polikarpov M A, Gabbasov R R and Yurenya A Y 2018 Separation of contributions of the magnetic relaxation and diffusion of nanoparticles in ferrofluids by analyzingthe hyperfine structure of Mössbauer spectra *JETP Lett.* **108** 59–62
[23] Bødker F and Mørup S 2000 Size dependence of the properties of hematite nanoparticles *Europhys. Lett.* **52** 217
[24] Plachinda A S, Sedov V E, Khromov V I, Suzdalev I P, Goldanskii V I, Nienhaus G U and Parak F 1992 Mössbauer studies of bound diffusion in model polymer system *Phys. Rev.* B **45** 7716
[25] Nowik I, Cohen S G, Bauminger E R and Ofer S 1983 Mössbauer absorption in overdamped harmonically bound particles in brownian motion *Phys. Rev. Lett.* **50** 1528
[26] Bonchev T, Vassilev I, Sapundzhiev T and Evitimov M 1968 Possibility of investigating movement in a group of ants by the Mössbauer effect *Nature* **217** 96
[27] Filipe V, Hawe A and Jiskoot W 2010 Critical evaluation of nanoparticle tracking analysis (NTA) by NanoSight for the measurement of nanoparticles and protein aggregates *Pharmac. Res.* **27** 796
[28] D'Arrigo J S 1978 Screening of membrane surface charges by divalent cations: an atomic representation *Am. J. Physiol., Cell Physiol.* **235** C109
[29] Hynes R C and Page Y L 1991 Sucrose, a convenient test crystal for absolute structures *J. Appl. Crystallogr.* **24** 352
[30] Kadoya K, Matsunaga N and Nagashima A 1985 Viscosity and thermal conductivity of dry air in the gaseous phase *J. Phys. Chem. Ref. Data* **14** 947

[31] Majka M and Góra P F 2017 Collective in diffusion of colloidal particles: from effective interactions to spatially correlated noise *J. Phys. A: Math. Theor.* **50** 054004